Structural Analysis of Chiral Complexes of Palladium(0) with 15-Membered Triolefinic Macrocyclic Ligands

Anna Pla-Quintana,[a] Anna Roglans,*[a] J. Vicente de Julián-Ortiz,[a] Marcial Moreno-Mañas,[b] Teodor Parella,*[c] Jordi Benet-Buchholz,*[d] and Xavier Solans[e]

Abstract: The complete structural analysis of the palladium complexes of the triolefinic macrocycles (*E,E,E*)-1,6,11-tris(arylsulfonyl)-1,6,11-triazacyclopentadeca-3,8,13-trienes, which featured from three identical to three different aryl groups, was achieved by performing X-ray diffraction studies, NMR spectroscopy, and other calculations. The stereochemical complexity is determined by the different isomers formed through complexation of the metal to one or other face of each of the three olefins involved. The palladacyclopropane formulation of the palladium–olefin interaction offers a clear picture of the stereogenicity of the olefin carbon atoms that are complexed to the metal. The energetically favorable isomers were identified in the solid-state and in solution by performing X-ray diffraction and NMR spectroscopic analysis, respectively.

Keywords: alkene ligands · macrocycles · palladium · stereoisomers · structure elucidation

Introduction

Palladium(0) complexes with dienes and trienes have been well characterized.[1] In addition, the advantages offered by the binding abilities of olefins to palladium(0) have been exploited; for example, $[Pd_2(dba)_4]$ and $[Pd_2(dba)_3]$·solvent are commercial sources of palladium(0) and are useful as catalysts or precatalysts in many chemical transformations. Several structural studies have reported on palladium complexes with alkenes that can exist as mixtures of isomers.[2] Among them, only those described by Pörschke and coworkers[2a] and those concerning $[Pd_2(dba)_3]$[2b] have no ligands other than olefins (Figure 1). This stereoisomerism is more apparent if the complex olefin–palladium(0) is represented as palladacyclopropane.

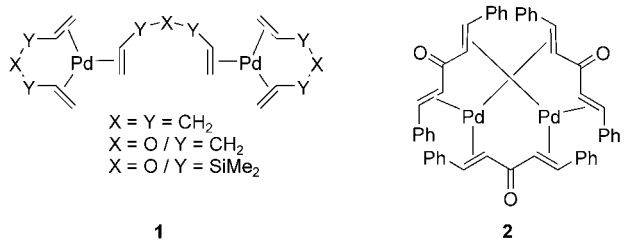

Figure 1. Palladium(0) complexes with olefins. For complex **1**, see reference [2a]; for complex **2**, see reference [2b].

[a] A. Pla-Quintana, Dr. A. Roglans, Dr. J. V. de Julián-Ortiz
Department of Chemistry, Universitat de Girona
Campus de Montilivi, 17071 Girona (Spain)
Fax: (+34) 972-418-150
E-mail: anna.roglans@udg.es

[b] Prof. Dr. M. Moreno-Mañas
Department of Chemistry, Universitat Autònoma de Barcelona
Cerdanyola, 08193 Barcelona (Spain)

[c] Dr. T. Parella
Servei de RMN, Universitat Autònoma de Barcelona
Cerdanyola, 08193 Barcelona (Spain)
Fax: (+34) 93-581-2291
E-mail: teodor.parella@uab.es

[d] Dr. J. Benet-Buchholz
Bayer Industry Services GMBH & Co. OHG
SUA-SPA X-ray Laboratory, Geb. Q18; Raum 66
51368 Leverkusen (Germany)
Present address: X-ray Diffraction Manager
Institut Català d'Investigació Química
Avda. Països Catalans s/n, 43007 Tarragona (Spain)
Fax: (+34) 977-920-224
E-mail: jbenet@iciq.es

[e] Prof. Dr. X. Solans
Department de Cristal·lografia
Mineralogia i Dipòsits Minerals, Universitat de Barcelona
Martí i Franquès s/n, 08028 Barcelona (Spain)

Supporting information for this article is available on the WWW under http://www.chemeurj.org/ or from the author.

 DOI: 10.1002/chem.200401073

As well as having an interesting structure, these complexes are also involved in several catalytic processes.[2d,3]

Some of us have previously described the preparation of 15-membered triolefinic macrocycles **3**[4] and their complexes with silver(I), platinum(0), and in particular, palladium(0) **4** (Figure 2).[4,5] Moreover, complexes **4** have been used as recoverable catalysts in Suzuki-type cross-couplings,[4a,d,f,g,6] telomerization of butadiene with methanol,[7] hydroarylation of alkynes in ionic liquids,[8] and the Mizoroki–Heck reaction.[9]

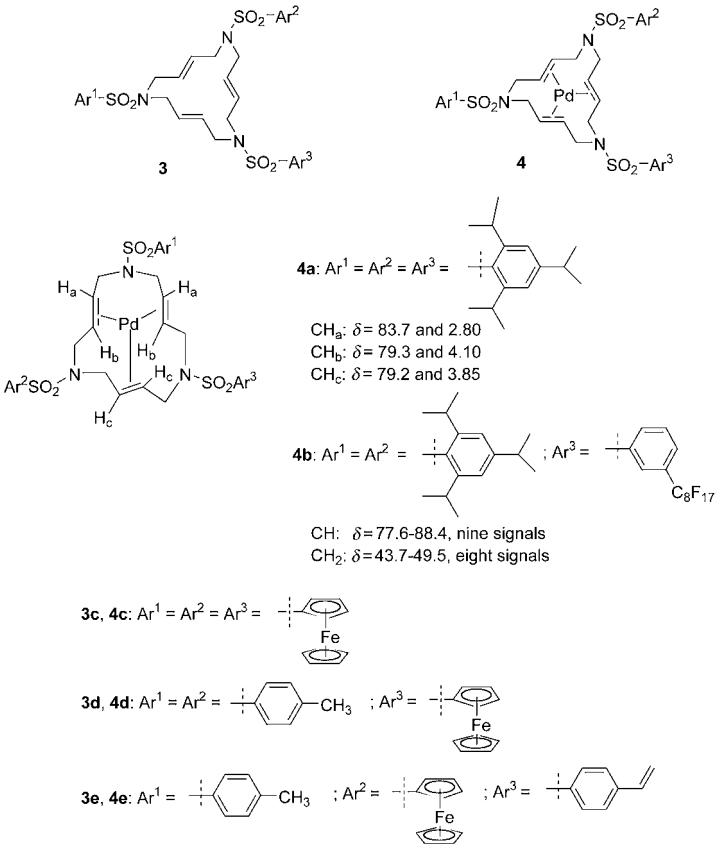

Figure 2. Structure of macrocyclic ligands **3** and their palladium complexes **4**. Data from preliminary NMR spectroscopy studies on the complexes **4a** and **4b** are also shown.

Abstract in Catalan: *Els complexos de pal·ladi de macrocicles triolefínics de tipus (*E,E,E*)-1,6,11-tris(arilsulfonil)-1,6,11-triazaciclopentadeca-3,8,13-triè, contenint des de tres unitats aríliques iguals fins a tres de diferents han estat estudiats mitjançant difracció de Raigs-X, espectroscòpia de RMN i càlculs teòrics. La complexitat estereoquímica deriva dels diferents isomers que es poden formar degut a la complexació del metall amb cadascuna de les dues cares de les tres olefines. La representació dels enllaços metall-olefina com a pal·ladaciclopropans permet una visualització més senzilla de l'estereoquímica dels àtoms de carboni olefínics després de la complexació. Els isomers energèticament possibles han estat determinats en l'estat sòlid i en solució mitjançant difracció de Raigs-X i espectroscòpia de RMN respectivament.*

The structure of palladium complexes **4** has intrigued us since their serendipitous discovery.[10] As an example, significant ^{13}C and ^{1}H NMR spectroscopy data for **4a** are summarized in Figure 2. The two olefinic CH groups that are located on opposite sides of one nitrogen atom in the ring (CH_a in Figure 2) give the same signals at $\delta = 83.7$ and 2.80 ppm. This also applies to the second set of olefinic CH groups (CH_b in Figure 2), which are directly linked to the previous pair, and absorb at $\delta = 79.3$ and 4.10 ppm. The CH groups of the third pair (CH_c in Figure 2) are magnetically equivalent and give only one signal at $\delta = 79.2$ and 3.85 ppm. This pattern was maintained for all the palladium(0) and platinum(0) complexes studied that featured three identical aryl groups.[4f,g] These results indicated that the C_3 axis in the free macrocycle **3a** disappeared and that a new type of symmetry was present. Thus, NMR spectroscopic studies suggested that this phenomenon was applicable to many other macrocyclic complexes, and, in addition, X-ray diffraction analysis again revealed loss of the C_3 axis.[5,6]

This raised the possibility of isomers in **4**, in which $Ar^1 = Ar^2 \neq Ar^3$, depending on whether the symmetry element can be maintained or whether it is broken by the different aryl substitutions. By addressing this problem,[5] we found for compound **4b** a set of nine signals of equal intensity at $\delta =$ 77.6–88.4 ppm for the olefinic carbon atoms, confirming the existence of different isomers.

Based on the chirality introduced in an olefin upon coordination to a metal,[11] we present here a complete structural analysis of compounds **4** (**4c**, **4d**), including those macrocycles with three different substituents (**4e**).

Results and Discussion

The general structure of all possible stereoisomers, resulting from coordination of the metal center to the two olefin faces of each double bond in the macrocycle, is depicted in Figure 3. Because the six olefinic carbon atoms become stereogenic upon coordination of the double bonds to the palladium(0),[11] the whole complex is chiral. Theoretically, 64 stereoisomers should be possible because there are six asymmetric carbon atoms; however, because all three double bonds are *trans*, the stereochemistry of one of the double-bond carbon atoms determines the stereochemistry of its partner, with the result that only three independent asymmetric centers can be considered. Therefore, only eight possible stereoisomers are feasible and these are grouped into four pairs of enantiomers (**A1**/**A2**, **A3**/**A4**, **A5**/**A6**, and **A7**/**A8** in Figure 3), in which each pair exhibits identical NMR spectroscopic properties.

The incorporation of the palladium nucleus into these triolefinic macrocyles introduces a high rigidity to the overall structure. This is confirmed by the absence of substantial chemical shift or line-shape variations, the absence of chemical exchange cross-peaks in NOESY spectra for a wide

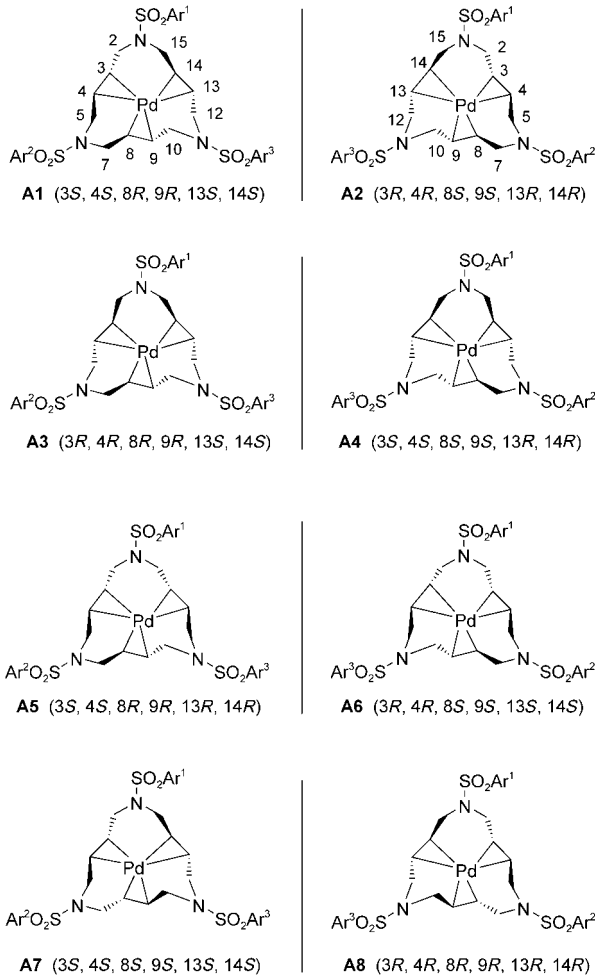

Figure 3. Stereoisomers for palladium(0) complexes **4** displayed as pairs of enantiomers.

range of temperatures, and the well-defined chemical shifts shown for the diastereotopic methylene protons. These observations do not support a process that exchanges the olefin face coordinated to palladium, even though several palladium(0) complexes with fluxional behavior have been described.[2]

The conversion between stereoisomers would imply the semirotation of a double bond, with an intermediate conformation in which the palladium atom lies just in the π-bond symmetry plane. To obtain a minimal estimation for such a barrier, the complex Pd–C_2H_4 was studied. Table 1 gives the energies calculated for different rotation angles with respect to the equilibrium conformation. Thus, 90° represents the maximal energy conformation, in which the palladium atom is coplanar to the ethylene molecule.

The rotational barrier for the Pd–C_2H_4 complex is calculated to be 27.45 kcal mol^{-1}, which is an inferior limit for the energy required for the interconversion of stereoisomers. Thus, such interconversion is energetically unfavorable.

The structure of these complexes can be regarded as alternated and fusioned three- and six-membered rings, in which the palladium belongs to all of these rings. Due to the *trans* configuration of the original double bond and, therefore, the corresponding three-membered ring, two different distributions should be possible: one with an energetically favourable *chair–chair–twist* (*cct*) conformation, and the other with an unfavourable *twist–twist–twist* (*ttt*) conformation (Figure 4), which has not been detected experimentally (see below).

Table 1. Energies calculated for different rotation angles with respect to the equilibrium conformation in Pd–C_2H_4.

Rotation angle [°][a]	Energy UB+HF–LYP [Hartrees/particle]	Energy excess [Hartrees/particle]	Energy excess [kcal mol^{-1}]
0	−205.3322946	0.00000000	0.00
15	−205.3249226	0.00737208	4.62
30	−205.3138673	0.01842731	11.56
45	−205.3021246	0.030170065	18.93
60	−205.2931904	0.039104217	24.54
75	−205.2893293	0.042965336	26.96
90	−205.2885465	0.043748125	27.45

[a] To obtain an estimate of the barrier of rotation of palladium around a double bond, the simple system Pd–C_2H_4 was taken. Geometries were minimized at B3LYP/LanL2DZ level by forcing the rotation angle to be 0, 15, 30, 45, 60, 75, and 90°, with respect to the equilibrium conformation.

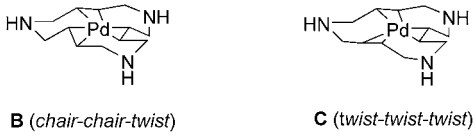

Figure 4. Simplified model structures for *cct* (**B**) and *ttt* (**C**) conformations.

Calculations designed to enable modeling of this complex [12] were performed on the simplified systems **B** and **C**, as experimental values of the energy required to change the conformations from **B** to **C** were not available. Density functional theory (DFT) calculations provided estimates of free energy differences, from which the conformational energies could be determined. The sum of the electronic and thermal free energies for each conformation revealed that structure **B** was 10.04 kcal mol^{-1} more stable than **C**. This difference is sufficient to indicate that only **B** would be detected experimentally, and because it is unlikely that the difference in free energies of the substituted structures would be less than that of these simplified ones, this conclusion should also be valid for the substituted species.

The substitution pattern at the nitrogen position in the ligand moiety defines the equivalence and, therefore, the symmetry of the various potential isomers. Thus, in the case of different substituents, different stereoisomers with different symmetry elements are possible (Table 2).

The nature of the palladium-containing three-membered ring is confirmed by the upfield proton and carbon chemical shift observed of the pseudo-olefinic centers (around $\delta =$ 2.75–4 and 78–83 ppm, respectively). The rigidity of the palladium-containing six-membered rings is high enough to

Table 2. Symmetry elements of the different stereoisomers of Figure 3 as a function of the substitution pattern.

Stereoisomers	$Ar^1=Ar^2=Ar^3$	$Ar^1=Ar^2\neq Ar^3$	$Ar^1\neq Ar^2\neq Ar^3$
A1/**A2**	C_2 axis[a]	none[b]	none
A3/**A4**	C_2 axis[a]	none[b]	none
A5/**A6**	C_2 axis[a]	C_2 axis	none
A7/**A8**[c]	C_3 axis+3 C_2 axes	C_2 axis	none

[a] **A1**, **A4**, and **A6** are the same molecule. [b] **A1** and **A4** are the same molecule. [c] Never observed experimentally.

avoid fluxional behavior and to permit easy differentiation between axial and equatorial protons. The overall *cct* conformation is confirmed by the presence of downfield olefinic resonances at $\delta=82$–83 ppm ($\delta=2.80$ ppm for proton), belonging to the *twist* conformation, and two similar upfield resonances at around $\delta=78$–79 ppm ($\delta=4.10$ and 3.9 ppm for protons), belonging to the *chair* conformations. This is also corroborated by the chemical shifts of the methylene groups, for which clear differentiation is observed between axial ($\delta=1.5$–1.6 ppm) and equatorial ($\delta=4.6$–4.65 ppm) positions ($\delta=48$–49 ppm for carbon) in the case of the *chair* conformation, whereas resonances at $\delta=3.05$–3.07 and 4.5–4.7 ppm ($\delta=45$ ppm for carbon) in the corresponding pseudoaxial and equatorial positions, respectively, are observed

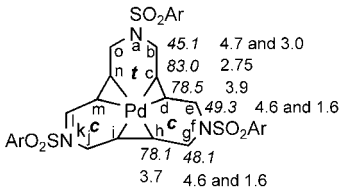

Figure 5. Averaged ^{1}H and ^{13}C NMR chemical shifts for palladium-complexed macrocycles showing the *cct* conformation. The carbon chemical shifts are shown in italics.

in the *twist* conformation (Figure 5). The *trans* stereochemistry in the palladacyclopropane ring is also confirmed by the large (11–12.5 Hz) proton–proton coupling constant between the pseudo-olefinic protons.

As a general trend, we observed that the region $\delta=78$–83 ppm in the conventional ^{13}C NMR spectra (Figure 6) is the most useful in analysis of these compounds, because the high degree of overlapping in the ^{1}H NMR spectra (Figure 7) or in other regions of the ^{13}C NMR spectra makes further analysis difficult. Complete ^{1}H and ^{13}C NMR chemical shift assignments are only possible by recording two-dimensional homonuclear and heteronuclear correlation spectra (Figure 8), with accurate high resolution and good signal-to-noise ratios, achieved by recording band-selective experiments and processing using linear prediction. In this way it was possible, for example, to distinguish between and to assign the poorly dispersed carbon resonances that appear in the interesting $\delta=78$–83 ppm region.

In the case of $Ar^1=Ar^2=Ar^3$ (**4c** in Figure 2), the compound consists of a pair of spectroscopically identical enantiomers with C_2 symmetry. This is confirmed in the

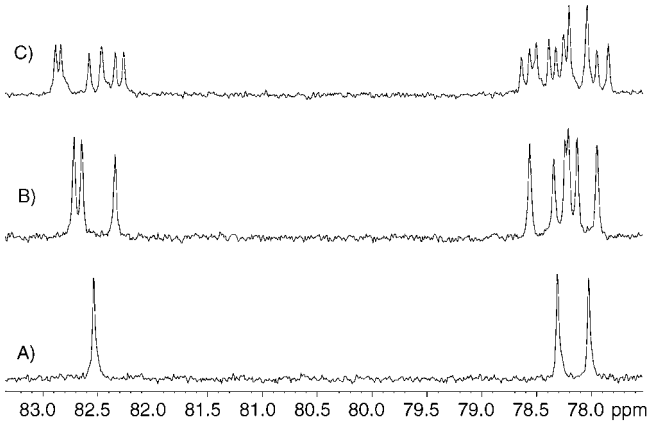

Figure 6. Expanded region of the ^{13}C NMR spectra (125.6 MHz) of A) **4c**, B) **4d**, and C) **4e**.

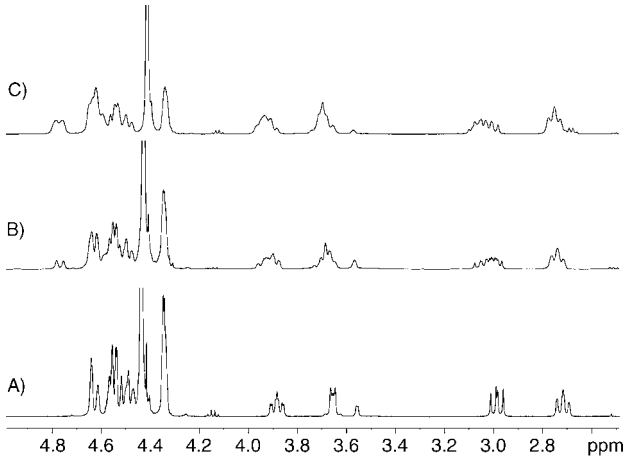

Figure 7. Aliphatic region of the ^{1}H NMR spectra (500 MHz) of A) **4c**, B) **4d**, and C) **4e**.

^{13}C NMR spectrum (spectrum A, Figure 6) by the presence of one separate resonance at $\delta=82.5$ ppm (*twist* conformation; ^{1}H NMR: $\delta=2.72$ ppm) and two close upfield resonances at $\delta=78.0$ and 78.3 ppm (*chair* conformation; ^{1}H NMR: $\delta=3.65$ and 3.88 ppm, respectively) of the same intensity. In the ^{1}H NMR spectrum (spectrum A in Figure 7), a total of 12 signals was expected. These are, however, only partially resolved. The *ttt* isomer with D_3 symmetry that should give rise to one olefinic ^{13}C NMR signal is clearly not present in solution.

For $Ar^1=Ar^2\neq Ar^3$ (**4d** in Figure 2), the NMR spectra are more complex. **A1** and **A4**, as well as **A2** and **A3**, have become identical and represent the enantiomers of the same molecule that does not have any symmetry element, whereas the enantiomers **A5**/**A6** have maintained their C_2 symmetry. The former isomer contributes six signals for olefinic carbon atoms (all 24 protons are inequivalent), and the latter furnishes three. In fact, a total of nine olefinic carbon resonances is found experimentally (spectrum B in Figure 6). The equal intensity of all signals indicates that the

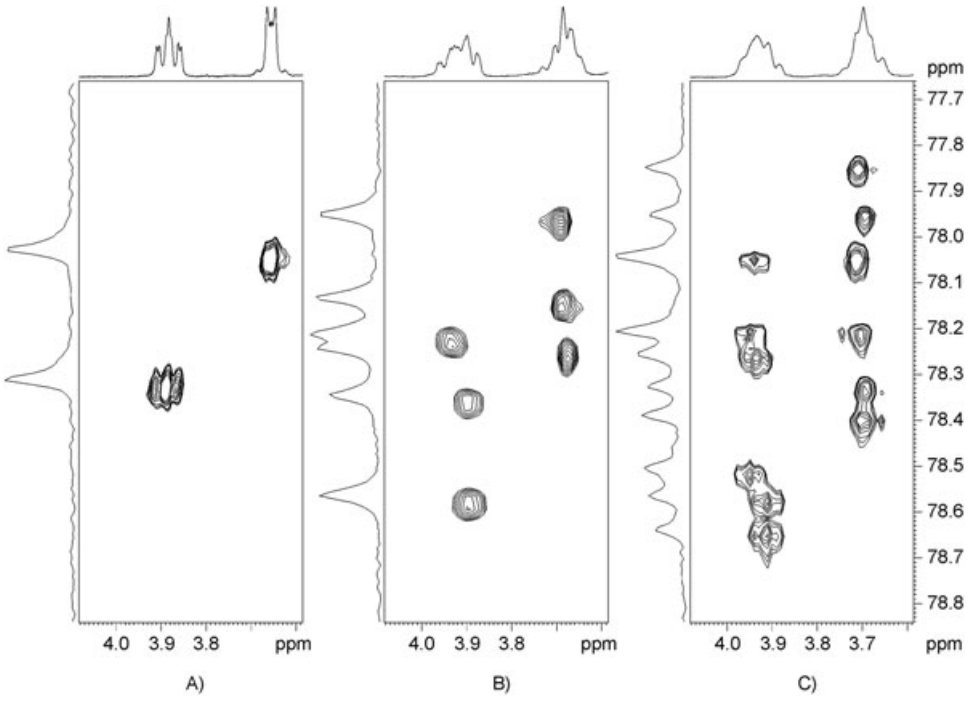

Figure 8. Expanded region of the ^{1}H–^{13}C HSQC correlation spectra (500 MHz) of A) **4c**, B) **4d**, and C) **4e**.

asymmetric isomer is present at twice the concentration of the C_2-symmetric isomer.[13]

For $Ar^1 \neq Ar^2 \neq Ar^3$ (**4e** in Figure 2), all three *cct* stereoisomers are present in equal proportions and, because they lack a symmetry element, each stereoisomer contributes six signals of equal intensity for olefinic carbon atoms. In practice, only 16 of the expected 18 signals are detected because two signals are degenerate (spectrum C in Figure 6 and the expanded $\delta = 77$–78 ppm region of spectrum C in Figure 8). In none of the cases were signals attributable to the hypothetical *ttt* isomers detected.

In Table 3, ^{1}H and ^{13}C NMR chemical shifts are given for ring signals of the experimentally observed stereoisomers of the palladium(0) complexes **4c**, **4d**, and **4e**.

Crystal structures: The crystal structures of the macrocyclic ligands **3c**, **3d**, and **3e** and their corresponding palladium complexes **4c**, **4d**, and **4e** were determined by performing single-crystal X-ray diffraction analysis. The molecular structure and the adopted numbering scheme are presented in Figure 9. Crystal data are listed in Tables 4 and 5, and selected bond lengths are given in Table 6.

The macrocyclic ligands **3c**, **3d**, and **3e** show a folded structure, with the planes of the three double bonds oriented randomly in different directions. In all three complexes **4c**, **4d**, and **4e**, the olefinic *trans* double bonds are coordinated to the palladium atom in a trigonal planar coordination geometry. The main deviations of the palladium atom from the plane defined by the central points of the three olefinic bonds (main plane) are 0.0033 Å for **4c**, 0.0009 Å for **4d** and 0.0023 Å for **4e**. By considering the standard deviations, the distances from the three double bonds to the palladium atom are identical for each compound.

As a result of the attractive interactions with the palladium atom, the planarity of the sp^2-hybridized carbon atoms

Table 3. ^{1}H and ^{13}C NMR spectroscopy data for complexes **4c**, **4d**, and **4e**.

Positions[a]	**4c**		**4d**				**4e**					
	A1/A2[b]		**A1/A2**[c]		**A5/A6**[b,d]		**A1/A2**[e]		**A3/A4**[f]		**A5/A6**[g]	
	^{1}H NMR	^{13}C NMR	^{1}H NMR	^{13}C NMR	^{1}H NMR	^{13}C NMR	^{1}H NMR	^{13}C NMR	^{1}H NMR	^{13}C NMR	^{1}H NMR	^{13}C NMR
b	4.61, 2.29	45.13	4.78, 3.07	45.11	4.64, 3.02	45.09	4.77, 3.05	45.00	4.63, 3.00	45.01	4.76, 3.04	45.08
c	2.72, –	82.54	2.78, –	82.6	2.77, –	82.91	2.763, –	82.34	2.750, –	82.83	2.752, –	82.26
d	3.88, –	78.31	3.97, –	78.34	3.97, –	78.56	3.935, –	78.04	3.932, –	78.25	3.905, –	78.61
e	4.49, 1.56	49.36	4.61, 1.64	49.41	4.61, 1.64	49.41	4.60, 1.62	49.33	4.60, 1.62	49.33	4.49, 1.58	49.23
g	4.49, 1.60	48.14	4.63, 1.70	48.18	4.63, 1.70	48.18	4.63, 1.67	48.10	4.63, 1.67	48.10	4.51, 1.62	47.99
h	3.65, –	78.02	3.73, –	78.26	3.73, –	78.16	3.707, –	78.04	3.703, –	77.84	3.689, –	78.32
i			3.71, –	78.44			3.695, –	78.39	3.698, –	78.20	3.689, –	77.95
j			4.52, 1.65	48.08			4.51, 1.63	47.99	4.63, 1.67	48.10	4.63, 1.67	48.10
l			4.50, 1.59	49.32			4.49, 1.58	49.23	4.60, 1.62	49.33	4.60, 1.62	49.33
m			3.93, –	78.69			3.905, –	78.54	3.945, –	78.51	3.944, –	78.29
n			2.78, –	82.55			2.756, –	82.58	2.750, –	82.88	2.756, –	82.46
o			4.78, 3.07	45.11			4.76, 3.04	45.11	4.63, 3.00	45.01	4.76, 3.06	45.08

[a] Lettering is depicted in Figure 5, taking as a reference the conformation of the six-membered rings. [b] Symmetric isomers, the values missing can be obtained by operating a C_2 symmetry. [c] This pair of enantiomers have a (ferrocenyl)sulfonyl unit on nitrogen k, and two (4-methylphenyl)sulfonyl units on nitrogens a and f. [d] This pair of enantiomers have a (ferrocenyl)sulfonyl unit on nitrogen a, and two equivalent (4-methylphenyl)sulfonyl units on nitrogens f and k. [e] This pair of enantiomers have a (4-methylphenyl)sulfonyl unit on nitrogen a, a (4-vinylphenyl)sulfonyl unit on nitrogen f, and a (ferrocenyl)sulfonyl unit on nitrogen k. [f] This pair of enantiomers have a (ferrocenyl)sulfonyl unit on nitrogen a, a (4-methylphenyl)sulfonyl unit on nitrogen f, and a (4-vinylphenyl)sulfonyl unit on nitrogen k. [g] This pair of enantiomers have a (4-vinylphenyl)sulfonyl unit on nitrogen a, a (ferrocenyl)sulfonyl unit on nitrogen f, and a (4-methylphenyl)sulfonyl unit on nitrogen k.

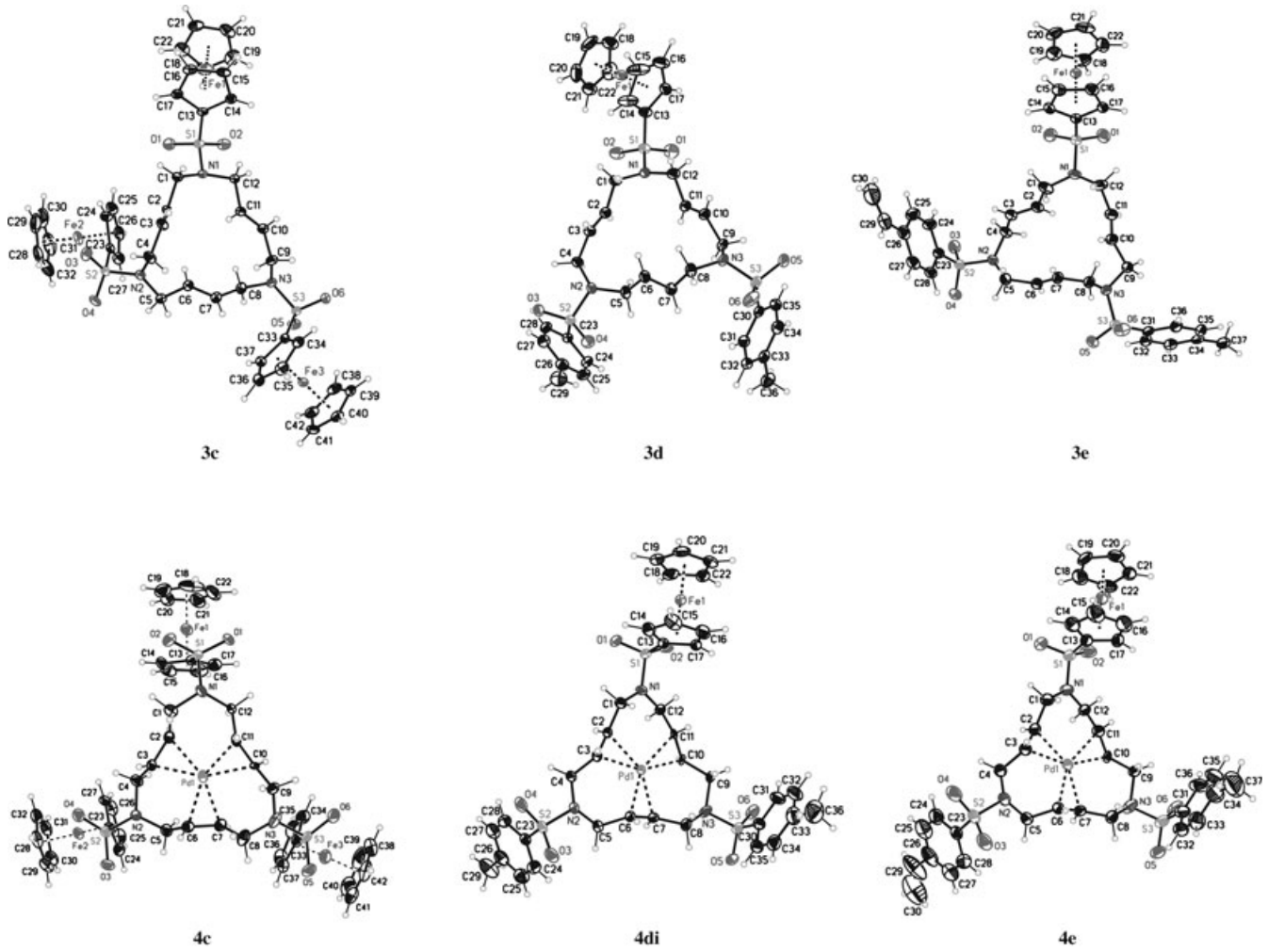

Figure 9. Ortep plots (50%) obtained from the X-ray crystallographic structural analyses of **3c**, **3d**, **3e**, **4c**, **4di**, and **4e**.

observed in the free ligands **3c**, **3d**, and **3e**, is lost in the corresponding complexes. Therefore, the olefinic substituents of the structures **4c**, **4d**, and **4e** are bent away from the palladium center by, on average, approximately 17°. The C–C bond lengths in the olefins are also elongated by an average of 0.055 Å upon coordination.

After complexation, the double bonds in **4c**, **4d**, and **4e** have fixed orientations with the palladium–alkene bond that are approximately perpendicular to the plane of the olefin. The three palladacyclopropane rings in these complexes create a three-paddled helix centered at the metal atom. Each of these three-membered rings is rotated through the palladium–alkene bond by approximately 20° with respect to the plane defined by the palladium atom and the central point of each olefin. The direction of this rotation cannot be inverted because it would imply an olefin face exchange and, consequently, breaking of the palladium–alkene coordination.

In the case of **4c** ($Ar^1 = Ar^2 = Ar^3$), according to Table 2, only two different pairs of enantiomers are possible (**A1**/**A2** and **A7**/**A8**). Complex **4c** crystallizes in a chiral space group in which one of the double bonds is disordered in two inverted positions in a 60:40 ratio. The two disordered positions correspond to the two different faces of the olefin coordinated to the palladium(0) atom. Both enantiomers **A1** and **A2** are obtained by selecting each one of the two disordered positions of the double bond, thus both compounds crystallize in the same crystal. Therefore, interchange of the disordered double bonds does not significantly modify the external morphology of the molecule. The chirality of the crystal is not derived from the palladacyclopropane rings, but from the asymmetrically fixed positions of the ferrocene substituents in the solid state. The C_2 symmetry detected in solution by using NMR spectroscopy is broken in the solid state by the fixed positions of the nitrogen substituents.

Compound **4d** crystallizes from dichloromethane as the main solvent, forming three different polymorphs/pseudopolymorphs **4di**, **4dii**, and **4diii**. These three crystal structures are centrosymmetric and differ in the orientation of the aryl substituents and, for **4diii**, in the number of solvent molecules in the crystal cell. Three different pairs of enantiomers are expected for **4d** ($Ar^1 = Ar^2 \neq Ar^3$), and only two of them

Table 4. Crystal data for compounds **3c**, **3d**, and **3e**.

Compound	**3c**	**3d**	**3e**
formula	$C_{42}H_{45}Fe_3N_3O_6S_3$	$C_{36}H_{41}FeN_3O_6S_3$	$C_{37}H_{41}FeN_3O_6S_3$
M_r	951.54	763.75	775.76
crystal size [mm^3]	4.0×4.0×0.4	2.0×1.0×0.5	0.04×0.08×0.10
crystal color	yellow	yellow	yellow
T [K]	153(2)	153(2)	153(2)
crystal system	monoclinic	triclinic	triclinic
space group	$P2_1/c$ (no. 14)	$P\bar{1}$ (no. 2)	$P\bar{1}$ (no. 2)
a [Å]	27.3192(7)	11.4559(3)	11.6184(3)
b [Å]	11.7145(3)	11.5887(3)	12.2852(3)
c [Å]	12.5458(3)	15.5168(4)	13.2667(4)
α [°]	90	98.4770(10)	97.1460(10)
β [°]	99.4090(10)	111.2890(10)	98.1250(10)
γ [°]	90	105.5290(10)	106.3160(10)
V [Å^3]	3961.03(17)	1779.38(8)	1772.07(8)
Z	4	2	2
ρ [g cm^{-3}]	1.596	1.425	1.454
μ [mm^{-1}]	1.296	0.650	0.654
θ_{max} [°]	31.50	31.55	31.52
reflns. measured	57045	27172	27356
unique reflns.	12564 [R_{int}=0.0517]	10921 [R_{int}=0.0492]	10898 [R_{int}=0.0572]
absorption correction	SADABS (Bruker)	SADABS (Bruker)	SADABS (Bruker)
transmission min/max	0.5590/1.0000	0.4635/1.0000	0.6976/1.0000
parameters	586	599	452
$R1/wR2$ [$I>2\sigma(I)$]	0.0403/0.0993	0.0450/0.1136	0.0478/0.1336
$R1/wR2$ [all data]	0.0574/0.1097	0.0535/0.1185	0.0604/0.1410
goodness-of-fit (F^2)	1.027	1.058	1.069
largest diff. peak/hole [e Å^{-3}]	1.587/−1.587	0.557/−0.651	1.554/−0.851

are detected by means of NMR spectroscopy (**A1**/**A2** and **A5**/**A6**). As in the former case (**4c**), structures **4di** and **4dii** crystallized so that one of the double bonds was disordered in two inverted positions with a 50:50 ratio for **4di** and a 61:39 ratio for **4dii**. In both cases, the disordered butene chain is situated next to Ar^3 (ferrocenyl). By selecting each one of the two disordered positions, the enantiomeric pair **A1**/**A2** or **A5**/**A6** is obtained. The structure **4diii** has no disorder at the double bond and it corresponds only to the enantiomeric pair **A5**/**A6**.

Only one centrosymmetrical crystalline form could be detected for compound **4e** by using dichloromethane as the crystallizing solvent. With Ar$^1 \neq$ Ar$^2 \neq$ Ar^3, there are three different pairs of favorable isomers (**A1**/**A2**, **A3**/**A4**, and **A5**/**A6**). Compound **4e** crystallizes with two disordered double bonds. The first one located between Ar^1 (*p*-methylphenyl) and Ar^2 (ferrocenyl) refines to a 50:50 ratio. The second disordered double bond located between Ar^2 (ferrocenyl) and Ar^3 (*p*-vinylphenyl) refines to a 90:10 ratio. By considering the refining ratios for both dis-

Table 5. Crystal data for compounds **4c**, **4d**, and **4e**.

Compound	**4c**	**4di**	**4dii**	**4diii**	**4e**
formula	$C_{42}H_{45}Fe_3N_3O_6PdS_3$·$2CH_2Cl_2$·$H_2O$	$C_{36}H_{41}FeN_3O_6PdS_3$·$CH_2Cl_2$	$C_{36}H_{41}FeN_3O_6PdS_3$·$CH_2Cl_2$	$C_{36}H_{41}FeN_3O_6PdS_3$·$2.5CH_2Cl_2$	$C_{37}H_{41}FeN_3O_6PdS_3$·$CH_2Cl_2$
M_r	1245.81	955.07	955.07	1082.46	663.80
crystal size [mm^3]	0.4×0.2×0.2	0.2×0.2×0.2	0.5×0.2×0.1	0.3×0.3×0.2	0.5×0.3×0.3
crystal color	yellow	yellow	yellow	yellow	yellow
T [K]	153(2)	153(2)	153(2)	153(2)	153(2)
crystal system	orthorhombic	triclinic	orthorhombic	monoclinic	triclinic
space group	$P2_12_12_1$ (no. 19)	$P\bar{1}$ (no. 2)	$Pbca$ (no. 61)	$P\bar{1}$ (no. 2)	$P\bar{1}$ (no. 2)
a [Å]	12.7092(3)	11.5144(3)	11.7532(4)	12.3845(2)	11.5284(3)
b [Å]	14.1875(3)	12.6773(3)	24.6364(9)	13.1334(3)	12.8895(3)
c [Å]	26.1318(6)	15.8112(4)	26.4924(10)	14.4093(3)	15.7731(4)
α [°]	90	93.5060(10)	90	94.040(1)	93.9930(10)
β [°]	90	105.4730(10)	90	105.666(1)	105.4510(10)
γ [°]	90	115.0380(10)	90	103.240(1)	115.1160(10)
V [Å^3]	4711.87(18)	1974.86(9)	7671.0(5)	2174.64(8)	2000.17(9)
Z	4	2	8	2	2
ρ [g cm^{-3}]	1.756	1.606	1.645	1.653	1.606
μ [mm^{-1}]	1.695	1.165	1.200	1.247	1.152
θ_{max} [°]	31.51	31.50	31.54	31.50	31.50
reflns. measured	67564	29527	104002	32618	30638
unique reflns.	14948 [R_{int}=0.0701]	11932 [R_{int}=0.0616]	12509 [R_{int}=0.1025]	13318 [R_{int}=0.0438]	12256 [R_{int}=0.0606]
absorption correction	SADABS (Bruker)	SADABS (Bruker)	SADABS (Bruker)	SADABS (Bruker)	SADABS (Bruker)
transmission min/max	0.5890/1.0000	0.6995/1.0000	0.6916/1.0000	0.6507/1.0000	0.5849/1.0000
parameters	675	512	517	617	581
Flack parameters	0.004(15)	–	–	–	
$R1/wR2$ [$I>2\sigma(I)$]	0.0520/0.1052	0.0491/0.1157	0.0465/0.0969	0.0556/0.1479	0.0498/0.1287
$R1/wR2$ [all data]	0.0622/0.1094	0.0676/0.1232	0.0822/0.1125	0.0618/0.1551	0.0647/0.1392
goodness-of-fit (F^2)	1.113	1.054	1.018	1.082	1.030
peak/hole [e Å^{-3}]	0.900/−1.533	1.052/−1.640	0.737/−1.057	1.476/−1.743	0.909/−1.369

Table 6. Selected bond lengths [Å] for compounds **3c**, **3d**, **3e**, **4c**, **4di**, **4dii**, **4diii**, and **4e**. Average lengths [Å] for bonds between disordered atoms are written in italics.

	3c	3d	3e	4c	4di	4dii	4diii	4e
C2–C3	1.320(3)	1.313(2)	1.321(3)	1.395(5)	1.381(4)	1.375(4)	1.393(4)	1.379(4)
C6–C7	1.326(3)	1.320(2)	1.313(3)	1.379(6)	1.376(4)	1.378(4)	1.385(4)	*1.363(4)*
C10–C11	1.325(3)	1.323(2)	1.311(3)	*1.37(2)*	*1.38(2)*	*1.39(2)*	1.384(4)	*1.38(3)*
Pd1–C2	–	–	–	2.192(4)	2.201(3)	2.196(3)	2.188(3)	2.200(3)
Pd1–C3	–	–	–	2.196(4)	2.206(3)	2.198(3)	2.199(3)	2.208(3)
Pd1–C6	–	–	–	2.206(4)	2.186(3)	2.197(3)	2.200(3)	*2.17(2)*
Pd1–C7	–	–	–	2.210(4)	2.181(3)	2.191(3)	2.203(3)	*2.23(5)*
Pd1–C10	–	–	–	*2.214(12)*	*2.190(7)*	*2.20(4)*	2.196(3)	*2.196(10)*
Pd1–C11	–	–	–	*2.23(5)*	*2.192(15)*	*2.196(6)*	2.165(3)	*2.198(9)*

ordered double bonds, 45% of the molecules belong to the enantiomeric pair **A1**/**A2**, 45% belong to the enantiomeric pair **A3**/**A4**, and 10% belong to enantiomeric pairs **A5**/**A6** and/or **A7**/**A8** (Figure 10). In light of the NMR spectroscopy data obtained, we hypothesize that the unfavorable *ttt* conformation is not formed, and that this 10% corresponds to the more favorable *cct* enantiomeric pair **A5**/**A6**.

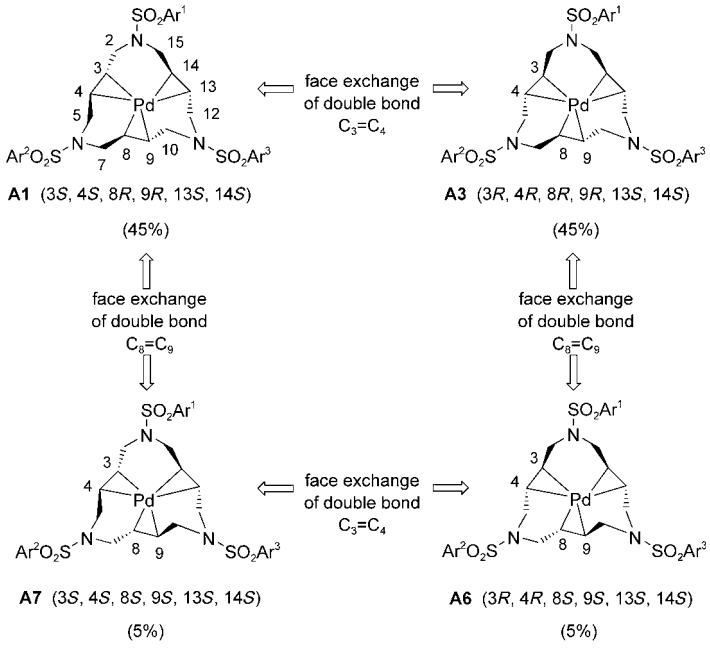

Figure 10. Distribution of stereoisomers in **4e**.

Conclusion

The palladium complexes of the triolefinic macrocycles (*E,E,E*)-1,6,11-tris(arylsulfonyl)-1,6,11-triazacyclopentadeca-3,8,13-trienes, featuring from three identical to three different aryl groups, exhibit a peculiar spectroscopic behavior. This behavior is intimately linked to the stereochemical complexity of the complexes. In turn, the stereochemical complexity stems from the different isomers that can be formed by complexation of the metal to one or other face of each of the three olefins involved. The palladacyclopropane formulation of the palladium–olefin interaction offers a clear picture of the stereogenicity of the olefin carbon atoms that are complexed to the metal. The various potential isomers have been determined in the solid state and in solution by performing X-ray diffraction and NMR spectroscopy studies, respectively. Calculations demonstrated that some theoretically possible isomers are too high in energy to exist, and that interconversions between existing isomers require transition barriers that are too great. Therefore, such dynamic processes do not occur, as confirmed by NMR spectroscopy data.

Experimental Section

NMR spectroscopy: High field ^{1}H and ^{13}C NMR analyses were conducted at the Servei de Ressonancia Magnetica Nuclear, Universitat Autònoma de Barcelona by using an AVANCE 500 BRUKER spectrometer for $CDCl_3$ solutions. Characterization of the compounds was performed by using typical gradient-enhanced 2D experiments, such as COSY, NOESY, HSQC, HSQC-TOCSY, and HMBC, recorded under routine conditions. For high-demand applications, band-selective 2D HSQC and HSQC-TOCSY experiments were carried out by applying a semiselective 180° pulse using a REBURP shape, instead of the conventional hard ^{13}C 180° pulse during the carbon evolution period. The selective pulse of 3 ms was implemented in a gradient spin-echo period to avoid the carbon evolution period during its application, and thus, achieves effective refocusing over the desired bandwith. In these experiments, 256 increments with 8 scans were applied for each t_1 value, and the spectral width was reduced in both dimensions to include only the resonances of interest. Data were finally processed by applying zero-filling and linear prediction to achieve full separation of all resonances.

Crystal structure determination

Preparation of crystals: Yellow crystals of **3c**, **3d**, **3e**, **4e**, **4di**, **4dii**, **4diii**, and **4e** were grown by the slow evaporation of dichloromethane/ethylacetate/hexane (1:1:1) solution under room temperature conditions. The crystals to be measured were prepared under inert conditions and immersed in perfluoropolyether as protecting oil for manipulation. CCDC 252093–252100 contain the supplementary crystallographic data for this paper. These data can be obtained free of charge from The Cambridge Crystallographic Data Centre via www.ccdc.cam.ac.uk/data_request/cif.

Data collection: Measurements were taken by using a Siemens P4 diffractometer equipped with a SMART-CCD-1000 area detector, a MACScience rotating anode with $Mo_{K\alpha}$ radiation, a graphite monochromator, and a Siemens LT2 low-temperature device ($T=-120$ °C). Full-sphere data collection was used with ω and ϕ scans. Programs used: data collection, Smart version 5.060 (Bruker AXS, 1999); data reduction, Saint+ version 6.02 (Bruker AXS, 1999); absorption correction, SADABS (Bruker AXS, 1999).

Structure solution and refinement: SHELXTL version 5.10 (Sheldrick, 1998) was used.[14]

Synthesis of macrocyclic derivatives 3 and their palladium(0) complexes 4: Compounds **3c**,[4d,f] **3d**,[4d,f,9] **4a**,[4a,f,5,8] **4b**,[4f,5] **4c**,[4d,f] and **4d**[4d,f,9] were prepared according to previously reported methods. Macrocycle **3e** and palladium(0) complex **4e** were synthesized by using modifications of the methods used for compounds **3** and **4**, respectively. Preparation and analytical data for **3e** and **4e** are available as Supporting Information.

Acknowledgements

Financial support from the MEC of Spain (projects BQU2002–04002 and BQU2003–01677), and the CIRIT-Generalitat de Catalunya (projects 2000SGR0062 and 2001SGR-00291) is gratefully acknowledged.

[1] a) D. Choueiry in *Handbook of Organopalladium Chemistry for Organic Synthesis, Vol. 1* (Ed.: E. Negishi), Wiley, New York, **2002**, pp. 147–187; b) R. Ugo, *Coord. Chem. Rev.* **1968**, *3*, 319–344; c) J. A. Davies in *Comprehensive Organometallic Chemistry II*, (Eds.: E. W. Abel, F. G. A. Stone, G. Wilkinson), Pergamon, **1995**, pp. 291–390; d) P. M. Maitlis, P. Espinet, M. J. H. Russell in *Comprehensive Organometallic Chemistry I*, (Eds.: G. Wilkinson, F. G. A. Stone, E. W. Abel), Pergamon, Oxford, **1982**, pp. 351–382 and pp. 455–469.

[2] For palladium(0) complexes with alkenes, see: a) J. Krause, G. Cestaric, K.-J. Haack, K. Seevogel, W. Storm, K.-R. Pörschke, *J. Am. Chem. Soc.* **1999**, *121*, 9807–9823; b) K. Selvakumar, M. Valentini, M. Wörle, P. S. Pregosin, A. Albinati, *Organometallics* **1999**, *18*, 1207–1215; for palladium(0) complexes with alkenes and phosphines, see: c) J. Krause, W. Bonrath, K.-R. Pörschke, *Organometallics* **1992**, *11*, 1158–1167; d) reference [2a]; e) B. R. Manzano, F. A. Jalón, F. Gómez-de la Torre, A. M. López-Agenjo, A. M. Rodríguez, K. Mereiter, W. Weissensteiner, R. Sturm, *Organometallics* **2002**, *21*, 789–802; f) J. P. Duan, F. L. Liao, S. L. Wang, C. H. Cheng, *Organometallics* **1997**, *16*, 3934–3940; for palladium(0) complexes with alkenes and P,N-ligands, see: g) F. Gómez de la Torre, F. A. Jalón, A. López-Agenjo, B. R. Manzano, A. Rodríguez, T. Sturm, W. Weissensteiner, M. Martínez-Ripoll, *Organometallics* **1998**, *17*, 4634–4644; h) F. A. Jalón, B. R. Manzano, F. Gómez de la Torre, A. M. López-Agenjo, A. M. Rodríguez, W. Weissensteiner, T. Sturm, J. Mahía, M. Maestro, *J. Chem. Soc. Dalton Trans.* **2001**, 2417–2424; i) reference [2b]; j) G. Bandoli, A. Dolmella, L. Crociani, S. Antonaroli, B. Crociani, *Transition Met. Chem.* **2000**, *25*, 17–25; for palladium(0) complexes with alkenes and N,N-ligands, see: k) R. van Asselt, C. J. Elsevier, W. J. J. Smeets, A. L. Spek, *Inorg. Chem.* **1994**, *33*, 1521–1531; l) M. W. van Laren, M. A. Duin, C. Klerk, M. Naglia, D. Rogolino, P. Pelagatti, A. Bacchi, C. Pelizzi, C. J. Elsevier, *Organometallics* **2002**, *21*, 1546–1553; m) M. L. Ferrara, F. Giordano, I. Orabona, A. Panunzi, F. Ruffo, *Eur. J. Inorg. Chem.* **1999**, 1939–1947.

[3] a) M. Gómez-Andreu, A. Zapf, M. Beller, *Chem. Commun.* **2000**, 2475–2476; b) F. Vollmüller, J. Krause, S. Klein, W. Mägerlein, M. Beller, *Eur. J. Inorg. Chem.* **2000**, 1825–1832; c) R. van Asselt, C. J. Elsevier, *J. Mol. Catal.* **1991**, *65*, L13–L19; d) R. van Asselt, C. J. Elsevier, *Organometallics* **1992**, *11*, 1999–2001; e) R. van Asselt, C. J. Elsevier, *Tetrahedron* **1994**, *50*, 323–334; f) A. Scrivanti, U. Matteoli, V. Beghetto, S. Antonaroli, B. Crociani, *Tetrahedron* **2002**, *58*, 6881–6886; g) A. Scrivanti, U. Matteoli, V. Beghetto, S. Antonaroli, R. Scarpelli, B. Crociani, *J. Mol. Catal. A* **2001**, *170*, 51–56; h) B. Crociani, S. Antonaroli, V. Beghetto, U. Matteoli, A. Scrivanti, *J. Chem. Soc. Dalton Trans.* **2003**, 2194–2202; i) reference [2b]; j) reference [2l].

[4] a) J. Cortès, M. Moreno-Mañas, R. Pleixats, *Eur. J. Org. Chem.* **2000**, 239–243; b) S. Cerezo, J. Cortès, D. Galvan, L. Lago, C. Marchi, E. Molins, M. Moreno-Mañas, R. Pleixats, J. Torrejón, A. Vallribera, *Eur. J. Org. Chem.* **2001**, 329–337; c) J. Cortès, M. Moreno-Mañas, R. Pleixats, *Tetrahedron Lett.* **2001**, *42*, 4337–4339; d) A. Llobet, E. Masllorens, M. Moreno-Mañas, A. Pla-Quintana, M. Rodríguez, A. Roglans, *Tetrahedron Lett.* **2002**, *43*, 1425–1428; e) M. Moreno-Mañas, J. Spengler, *Tetrahedron* **2002**, *58*, 7769–7774; f) M. Moreno-Mañas, R. Pleixats, A. Roglans, R. M. Sebastián, A. Vallribera, *Arkivoc* **2004**, 109–129 (http://www.arkat-usa.org); g) M. Moreno-Mañas, R. Pleixats, A. Roglans, R. M. Sebastián, A. Vallribera, *J. Organomet. Chem.* **2004**, *689*, 3669–3684; h) J. Masllorens, A. Roglans, M. Moreno-Mañas, T. Parella, *Organometallics* **2004**, *23*, 2533–2540.

[5] S. Cerezo, J. Cortès, E. Lago, E. Molins, M. Moreno-Mañas, T. Parella, R. Pleixats, J. Torrejón, A. Vallribera, *Eur. J. Inorg. Chem.* **2001**, 1999–2006.

[6] A. Llobet, E. Masllorens, M. Rodríguez, A. Roglans, J. Benet-Buchholz, *Eur. J. Inorg. Chem.* **2004**, 1601–1610.

[7] a) B. Estrine, B. Blanco, S. Bouquillon, F. Hénin, M. Moreno-Mañas, J. Muzart, C. Pena, R. Pleixats, *Tetrahedron Lett.* **2001**, *42*, 7055–7057; b) M. Moreno-Mañas, R. Pleixats, J. Spengler, C. Chevrin, B. Estrine, S. Bouquillon, F. Hénin, J. Muzart, A. Pla-Quintana, A. Roglans, *Eur. J. Org. Chem.* **2003**, 274–283.

[8] S. Cacchi, G. Fabrizi, A. Goggiamani, M. Moreno-Mañas, A. Vallribera, *Tetrahedron Lett.* **2002**, *43*, 5537–5540.

[9] J. Masllorens, M. Moreno-Mañas, A. Pla-Quintana, A. Roglans, *Org. Lett.* **2003**, *5*, 1559–1561.

[10] S. Cerezo, J. Cortès, J.-M. López-Romero, M. Moreno-Mañas, T. Parella, R. Pleixats, A. Roglans, *Tetrahedron* **1998**, *54*, 14885–14904.

[11] An olefinic compound without substituent asymmetric groups, and without symmetry planes perpendicular to the plane of the double bond, becomes asymmetric upon coordination. See: a) G. Paiaro, A. Panunzi, *J. Am. Chem. Soc.* **1964**, *86*, 5148–5152; b) G. Paiaro, *Organomet. Chem. Rev. Sect. A* **1970**, *6*, 319–335.

[12] Simplified structures presented here were taken from the X-ray crystallography-determined geometry, modified, first optimized by the UFF force field[12a], and finally optimized at the DFT level. The B3LYP hybrid functional proposed by Becke[12b] and a basis set of valence double ζ quality, were employed. Relativistic effects were implicitly addressed by the use of relativistic effective core potential (RECP) for palladium.[12c–e] The standard Dunning–Hay D95 V basis[12f] was used for H, C, and N. This combination of RECP and basis set is commonly denoted as LanL2DZ. Harmonic vibrational frequencies were calculated at the B3LYP level for the optimized geometries, and were used to obtain thermochemical data estimates. Calculations were performed by means of the Gaussian 98 package.[12g] a) A. K. Rappé, C. J. Casewit, K. S. Colwell, W. A. Goddard III, W. M. Skiff, *J. Am. Chem. Soc.* **1992**, *114*, 10024–10035; b) A. D. Becke, *J. Chem. Phys.* **1993**, *98*, 5648–5652; c) P. J. Hay, W. R. Wadt, *J. Chem. Phys.* **1985**, *82*, 270–283; d) W. R. Wadt, P. J. Hay, *J. Chem. Phys.* **1985**, *82*, 284–298; e) P. J. Hay, W. R. Wadt, *J. Chem. Phys.* **1985**, *82*, 299–310; f) T. H. Dunning, Jr., P. J. Hay in *Modern Theoretical Chemistry, Vol. 3*, (Ed.: H. F. Schaefer III), Plenum, New York, **1976**; g) Gaussian 98, (Revision A.9), M. J. Frisch, G. W. Trucks, H. B. Schlegel, G. E. Scuseria, M. A. Robb, J. R. Cheeseman, V. G. Zakrzewski, J. A. Montgomery, Jr., R. E. Stratmann, J. C. Burant, S. Dapprich, J. M. Millam, A. D. Daniels, K. N. Kudin, M. C. Strain, O. Farkas, J. Tomasi, V. Barone, M. Cossi, R. Cammi, B. Mennucci, C. Pomelli, C. Adamo, S. Clifford, J. Ochterski, G. A. Petersson, P. Y. Ayala, Q. Cui, K. Morokuma, D. K. Malick, A. D. Rabuck, K. Raghavachari, J. B. Foresman, J. Cioslowski, J. V. Ortiz, A. G. Baboul, B. B. Stefanov, G. Liu, A. Liashenko, P. Piskorz, I. Komaromi, R. Gomperts, R. L. Martin, D. J. Fox, T. Keith, M. A. Al-Laham, C. Y. Peng, A. Nanayakkara, M. Challacombe, P. M. W. Gill, B. Johnson, W. Chen, M. W. Wong, J. L. Andres, C. Gonzalez, M. Head-Gordon, E. S. Replogle, J. A. Pople, Gaussian, Inc., Pittsburgh, PA, **1998**.

[13] Identical spectroscopic behavior has been found for complex **4f** ($Ar^1 = Ar^2 \neq Ar^3$) bearing two ferrocenylsulfonyl units and one (4-methylphenyl)sulfonyl unit.

[14] G. M. Sheldrick, SHELXTL Crystallographic System Version 5.10, Bruker AXS Inc., Madison, Wisconsin, **1998**.

Received: October 21, 2004
Published online: February 25, 2005

